# A new steady-state gas/particle partitioning model of PAHs: Implication for the influence of the particulate proportion in emissions

Fu-Jie Zhu[a,b], Peng-Tuan Hu[a,c], Wan-Li Ma[a,b,*]

[a] International Joint Research Center for Persistent Toxic Substances (IJRC-PTS), State Key Laboratory of Urban Water Resource and Environment, Harbin Institute of Technology, Harbin 150090, China

[b] Heilongjiang Provincial Key Laboratory of Polar Environment and Ecosystem (HPKL-PEE), Harbin 150090, China

[c] School of Environment, Key Laboratory for Yellow River and Huai River Water Environment and Pollution Control, Ministry of Education, Henan Normal University, Xinxiang, China

*Corresponding author. International Joint Research Center for Persistent Toxic Substances (IJRC-PTS), State Key Laboratory of Urban Water Resource and Environment, Harbin Institute of Technology, 73 Huanghe Road, Nangang District, Harbin 150090, Heilongjiang, China.

Email address: mawanli002@163.com

**Abstract:**

Gas/particle (G/P) partitioning is an important atmospheric process for semi-volatile organic compounds (SVOCs). However, the exact prediction of the G/P partitioning ~~coefficients ($K_P$)~~ of polycyclic aromatic hydrocarbons (PAHs) was still a challenge. In this study, a new steady-state G/P partitioning model was established based on the level III multimedia fugacity model, with the introduction of the particulate proportion of PAHs in emission ($\phi_0$) particularly. Same with the previous steady-state model, three different domains with different G/P partitioning behaviors can be divided by the threshold values of log $K_{OA}$ (octanol-air partitioning coefficient), and the slopes of the prediction line of the new model were 1, from 1 to 0, and 0 for the three domains, respectively. The difference between the new steady-state model and previous G/P partitioning models was quite different in different domains. It was found that the deviation with the G/P partitioning~~$K_P$~~ of PAHs from the equilibrium state was caused by both the gaseous and particulate interferences, in which $\phi_0$ determined the influence of the two interferences. Different forms of the new steady-state model were observed under different values of $\phi_0$, indicating its important influence of G/P partitioning of PAHs. The comparison with the G/P partitioning~~log $K_P$~~ of PAHs between the prediction result of the new steady-state model and the monitored results from 11 cities in China suggested different prediction performances under different values of $\phi_0$ and the lowest root mean square error when $\phi_0$ was set to 0.9 or 0.99. The result indicated that the $\phi_0$ was an important factor for the G/P partitioning of PAHs. In addition, the new steady-state model also showed good performance for the prediction of ~~log $K_P$~~G/P partitioning of PAHs with totally gaseous emission and PBDEs with totally particulate emission. Therefore, it can be concluded that the $\phi_0$ should be considered in the study of G/P partitioning of PAHs, which also provided a new insight for other SVOCs.

## Graphical Abstracts

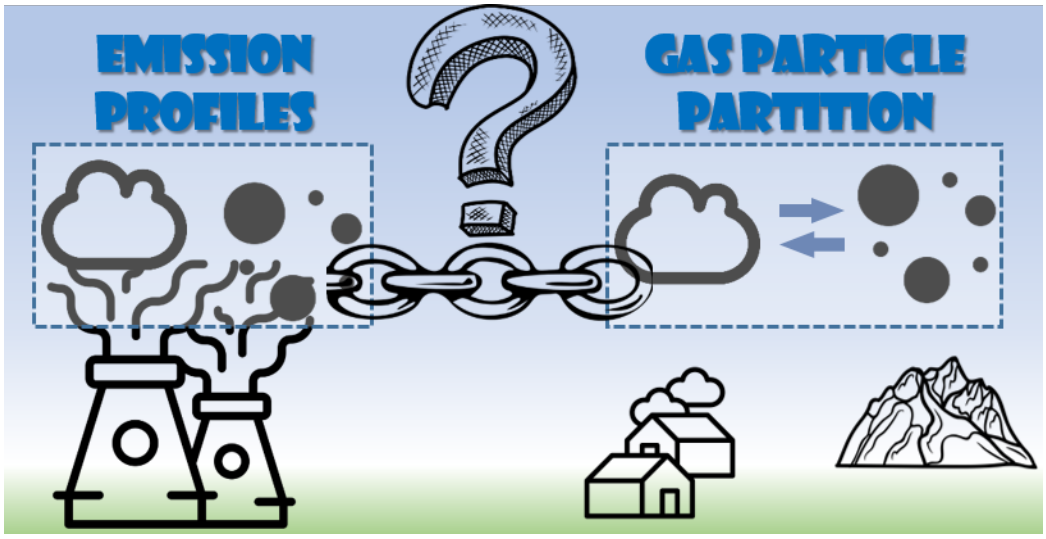

## 1. Introduction

Atmospheric long-range transport can move the semi-volatile organic compounds (SVOCs) from sources to remote regions, such as the Arctic and the Tibetan Plateau, where the SVOCs are not produced and used (Hung et al., 2005; Hung et al., 2010; Wang et al., 2018a). The gas/particle (G/P) partitioning of SVOCs is an important atmospheric process, which governs their long-range transport and fate in atmosphere (Zhao et al., 2020; Li et al., 2015). For example, the wet and dry depositions of SVOCs are controlled by the distribution between gas phase and particle phase, thus affecting the efficiency and scope of long-range transport from sources to remote regions (Bidleman, 1988). In addition, the routes of entering the human body are also different for gaseous and particulate SVOCs, which indicated that the G/P partitioning of SVOCs is also a significant issue for human exposure assessment (Weschler et al., 2015; Hu et al., 2021).

The G/P partitioning of SVOCs has been studied for decades, and some models were developed for the prediction of the G/P partitioning coefficient ($K_P$) of SVOCs (Zhu et al., 2021; Qiao et al., 2020). Recently, Qiao et al. (2020) summarized eight G/P partitioning models into three groups: (1) the models based on the equilibrium-state theory (Pankow, 1987; Harner and Bidleman, 1998; Dachs and Eisenreich, 2000; Goss, 2005), (2) the empirical models based on monitoring data (Li and Jia, 2014; Wei et al., 2017; Shahpoury et al., 2016), and (3) the models based on the steady-state theory (Li et al., 2015). In addition, a new empirical model (equation) for polycyclic aromatic hydrocarbons (PAHs) (Zhu et al., 2022) and a new steady-state mass balance model for polybrominated diphenyl ethers (PBDEs) (Zhao et al., 2020) have been established recently ~~for the prediction of $K_P$~~. In general, the effectiveness and performance of these models have been evaluated with field monitoring programs (Vuong et al., 2020; Qiao

et al., 2019), and these models have been frequently used for predicting the G/P partitioning behavior of SVOCs (Qiao et al., 2020).

Along with the concurrent formation of particle, the G/P partitioning process of PAHs was more complex than other SVOCs (Dachs and Eisenreich, 2000; Shahpoury et al., 2016; Zhu et al., 2021). For example, it was found that when the value of octanol-air partitioning coefficient (log $K_{OA}$) was more than 12, the monitored values of $K_{P\text{-}M}$ (monitoring data of G/P partitioning) of PAHs varied from both the predictions of the equilibrium-state G/P partitioning models and the steady-state G/P partitioning models (Ma et al., 2020; Zhu et al., 2021). Recent studies have found that the particulate proportion of SVOCs in the emissions ($\phi_0$) could affect the G/P partitioning of SVOCs (Qin et al., 2021; Zhao et al., 2020). For example, when $\phi_0$ increased, the predictions could diverge from the steady-state G/P partitioning model to the equilibrium-state G/P partitioning model (Qin et al., 2021; Zhao et al., 2020). Furthermore, the emission sources of PAHs in atmosphere are complex, including stationary sources (residential combustion, industrial production and agricultural burning) and mobile sources (motor vehicles, railways, and shipping) (Zhang et al., 2020; Tang et al., 2020), in which the gaseous and particulate PAHs both exist (Zimmerman et al., 2019; Wang et al., 2018b; Shen et al., 2011; Cai et al., 2018b). Therefore, the detailed influence of $\phi_0$ on the G/P partitioning of PAHs might be considered for the deviation of the measured $K_{P\text{-}M}$ from both the equilibrium-state G/P partitioning model and the steady-state G/P partitioning model predictions.

In this study, a new steady-state G/P partitioning model (called the new steady-state model for short hereafter) was established based on the level III multimedia fugacity model for PAHs, and the influence of $\phi_0$ of PAHs in emissions was comprehensively discussed. The following topics were conducted: (1) the new steady-

state model was established and deeply studied under different threshold values of log $K_{OA}$; (2) the influence of $\phi_0$ on the G/P partitioning of PAHs was comprehensively discussed; and (3) the performance of the new steady-state model for the prediction of $K_{P\text{-}M}$ of PAHs were discussed finally.

## 2. Establishment of the new steady-state G/P partitioning model

### 2.1. Establishment method of the new steady-state model

A steady-state six-compartment six-fugacity model was applied in the present study, which can be found in detail in **Text S1, Supporting Information (SI)**. The input and output fluxes of gas phase and particle phase PAHs were presented in **Fig. 1**. The detailed calculation methods for these fluxes can be found in **Text S2, SI**.

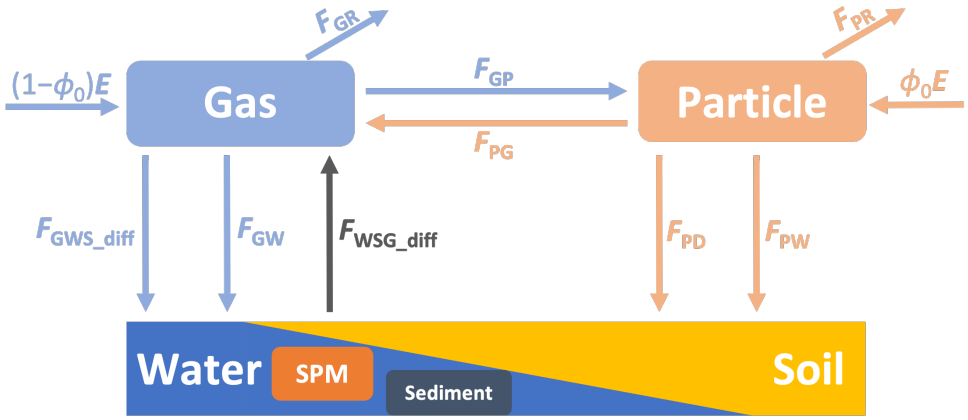


Fig. 1. The fluxes related to the gas and particle phase in the six-compartment model (Note: $F_{GR}$: degradation flux of gas phase PAHs; $F_{PR}$: degradation flux of particle phase PAHs; $F_{GP}$: migration flux from gas phase to particle phase; $F_{PG}$: migration flux from particle phase to gas phase; $F_{GWS\_diff}$: diffusion fluxes from gas phase to water and/or soil phases; $F_{GW}$: wet deposition flux of gas phase PAHs to water and/or soil phase; $F_{WSG\_diff}$: diffusion fluxes from soil and/or water phases to gas phase; $F_{PD}$: dry deposition flux of particle phase PAHs to SPM and/or soil phase; $F_{PW}$: wet deposition flux of particle phase PAHs to SPM and/or soil phase; $(1-\phi_0)E$: emission flux of gas phase PAHs; $\phi_0 E$: emission flux of particle phase PAHs.)

The input and output fluxes of gas phase and particle phase were compared in four groups (input fluxes of gas phase, output fluxes of gas phase, input fluxes of particle phase, and output fluxes of particle phase), and the results for PAHs were presented in **Fig. S1, SI**. In the present study, in order to establish a universal and simple model, the four fluxes ($F_{GWS\_diff}$, $F_{WSG\_diff}$, $F_{PR}$, and $F_{GW}$) were removed from the system because their contributions were less than 10% of the total fluxes. In addition, the special situation was not considered, for example, even the contribution of the flux of $F_{GW}$ for DahA was higher than 10%, the $F_{GW}$ was also removed.~~It can be found that the four fluxes ($F_{GWS\_diff}$, $F_{WSG\_diff}$, $F_{PR}$, and $F_{GW}$) can be removed from the system due to their ignored proportion in each group.~~ After simplifying the function in **Text S1, SI**, the two linear equations describing the input and output fluxes of gas phase and particle phase can be established as follows:

$$\begin{cases} (1-\phi_0)E + D_{GP}f_P = (D_{GR} + D_{GP})f_G \\ \phi_0 E + D_{GP}f_G = (D_{GP} + D_{PD} + D_{PW})f_P \end{cases} \quad (1)$$

where, $f_P$ is the fugacity for particle phase; $f_G$ is the fugacity for gas phase; $D_{GP}$ is the intermedia $D$ value between gas phase and particle phase; $D_{GR}$ is the $D$ value for the degradation of gas phase PAHs; $D_{PD}$ and $D_{PW}$ are the $D$ values of the dry and wet depositions of particle phase PAHs, respectively.

The fugacity ratio of the particle phase to the gas phase can be obtained by solving the Eq. (1) as follows:

$$\frac{f_P}{f_G} = \frac{D_{GP}+\phi_0 D_{GR}}{D_{GP}+(1-\phi_0)(D_{PD}+D_{PW})} \quad (2)$$

According to ~~the calculation method of log $K_P$ from~~ the fugacity method (Li et al., 2015) (See details in **Text S3, SI**), the new steady-state model can be expressed as follows:

$$\log K_{\mathrm{P-NS}} = \log K_{\mathrm{P-HB}} + \log\left(\frac{D_{\mathrm{GP}}+\phi_0 D_{\mathrm{GR}}}{D_{\mathrm{GP}}+(1-\phi_0)(D_{\mathrm{PD}}+D_{\mathrm{PW}})}\right) \quad (3)$$

In the Eq. (3), the log $K_{\text{P-HB}}$ is the equilibrium-state G/P partitioning model (named as the H-B model in this study, log $K_{\text{P-HB}}$ = log $K_{\text{OA}}$ + log $f_{\text{OM}}$ −11.91, and $f_{\text{OM}}$ is the fraction of organic matters in particles) (Harner and Bidleman, 1998). The part of $D_{\text{GR}}$, caused by the degradation of PAHs in gas phase, is defined as the gaseous interference, and the part of $D_{\text{PD}}$ + $D_{\text{PW}}$, caused by the deposition of PAHs in particle phase, is defined as the particulate interference. Therefore, the levels of the influences of the two interferences were based on the value of $\phi_0$.

By applying the calculation method of the $D$ values in the multimedia fugacity model (**Table S1, SI**) and the values of the related parameters in the **Tables S2, S3, S4, S5, and S6, SI**, the Eq. (2) can be simplified as follows:

$$\frac{f_{\mathrm{P}}}{f_{\mathrm{G}}} = \frac{1+13.2\phi_0\times k_{\mathrm{deg}}}{1+10^{-10.31}(1-\phi_0)f_{\mathrm{OM}}K_{\mathrm{OA}}} \quad (4)$$

where, $k_{\text{deg}}$ is the degradation rate of PAHs in gas phase ($h^{-1}$); and $K_{\text{OA}}$ is the octanol-gas partitioning coefficient.

Therefore, the Eq. (3) can be also expressed as follows:

$$\log K_{\mathrm{P-NS}} = \log K_{\mathrm{P-HB}} + \log\left(\frac{1+13.2\phi_0\times k_{\mathrm{deg}}}{1+10^{-10.31}(1-\phi_0)f_{\mathrm{OM}}K_{\mathrm{OA}}}\right) \quad (5)$$

Thus, it can be found that the new steady-state model (log $K_{\text{P-NS}}$) is a function of $\phi_0$, $k_{\text{deg}}$, $f_{\text{OM}}$ and $K_{\text{OA}}$.

## 2.2. Different domains of the new steady-state model

Three domains were identified according to the threshold values of log $K_{\text{OA}}$. For example, if $10^{-10.31}(1-\phi_0)f_{\text{OM}}K_{\text{OA}} \ll 1$, the first threshold of log $K_{\text{OA}}$ (log $K_{\text{OA1}}$) can be obtained. Then, the Eq. (5) is expressed as follows:

$$\log K_{\mathrm{P-NS}} = \log K_{\mathrm{P-HB}} + \log\left(1 + 13.2\phi_0 \times k_{\mathrm{deg}}\right) \quad (6)$$

In this domain, the value of log $K_{OA}$ was less than log $K_{OA1}$, and the log $K_{P\text{-}NS}$ was related to $K_{OA}$, $f_{OM}$, $\phi_0$ and $k_{deg}$. The domain was presented with vertical lines as background in **Fig. 2**. In this domain, the prediction line of the new steady-state model was parallel with that of the H-B model.

In addition, if $10^{-10.31}(1-\phi_0)f_{OM}K_{OA} >> 1$, the second threshold of log $K_{OA}$ (log $K_{OA2}$) can be obtained. The Eq. (5) is expressed as follows:

$$\log K_{\mathrm{P-NS}} = \log K_{\mathrm{P-HB}} + \log\left(\frac{1+13.2\phi_0\times k_{\mathrm{deg}}}{10^{-10.31}(1-\phi_0)f_{\mathrm{OM}}K_{\mathrm{OA}}}\right) \quad (7)$$

By substituting the log $K_{P\text{-}HB}$ using the equation (log $K_{P\text{-}HB}$ = log $K_{OA}$ + log $f_{OM}$ −11.91) (Harner and Bidleman, 1998), the Eq. (7) can be simplified as follows:

$$\log K_{\mathrm{P-NS}} = \log\left(\frac{1+13.2\phi_0\times k_{\mathrm{deg}}}{1-\phi_0}\right) - 1.6 \quad (8)$$

In this domain, the value of log $K_{OA}$ was higher than log $K_{OA2}$, the log $K_{P\text{-}NS}$ was only related to $\phi_0$ and $k_{deg}$, and the log $K_{P\text{-}NS}$ will be a maximum constant (log $K_{P\text{-}NSmax}$), as the part with horizontal lines as background in **Fig. 2**. In this domain, the prediction line of the new steady-state model was parallel with that of the L-M-Y model.

Furthermore, when log $K_{OA1}$ < log $K_{OA}$ < log $K_{OA2}$, the log $K_{P\text{-}NS}$ increased along with the increasing of log $K_{OA}$, and the increasing rate (or the slope of the function of log $K_{P\text{-}NS}$ (Eq. 5)) decreased from 1 to 0. The log $K_{P\text{-}NS}$ was related to $K_{OA}$, $f_{OM}$, $\phi_0$ and $k_{deg}$. This domain was presented as the part in with diagonal lines as background **Fig. 2**. In this domain, the prediction line of the new steady-state model was similar with that of the L-M-Y model.

### 2.3. Difference between of the new steady-state model and other previous models

The difference between the new steady-state model with the H-B model (**Text S4, SI**) and the L-M-Y model (the steady-state model) (Li et al., 2015) (**Text S4, SI**) can

be calculated by the Eq. (5) in different domains. Briefly, as shown in **Fig. 2**, when log $K_{OA}$ < log $K_{OA1}$, the difference between the new steady-state model and the H-B model or the L-M-Y model can be expressed as $\delta_1$ = log (1 + 13.2$\phi_0$ × $k_{deg}$). The value of $\delta_1$ increased along with the increase of $\phi_0$, and will reach the maximum value of log (1 + 13.2$k_{deg}$) when $\phi_0$ = 1 (**Fig. S2a, SI**). When log $K_{OA}$ > log $K_{OA2}$, the difference between the new steady-state model and the L-M-Y model can be expressed as $\delta_2$ = log [(1 + 13.2$\phi_0$ × $k_{deg}$) / (1 − $\phi_0$)]. The value of $\delta_2$ also increased along with the increase of $\phi_0$, and will approach infinity when $\phi_0$ infinitely close to 1 (**Fig. S2b, SI**). When log $K_{OA1}$ < log $K_{OA}$ < log $K_{OA2}$, the difference between the new steady-state model and the L-M-Y model was the function of $\phi_0$ and $K_{OA}$, which increased along with the increasing of $\phi_0$ and $K_{OA}$, and more detailed information can be found in next section.

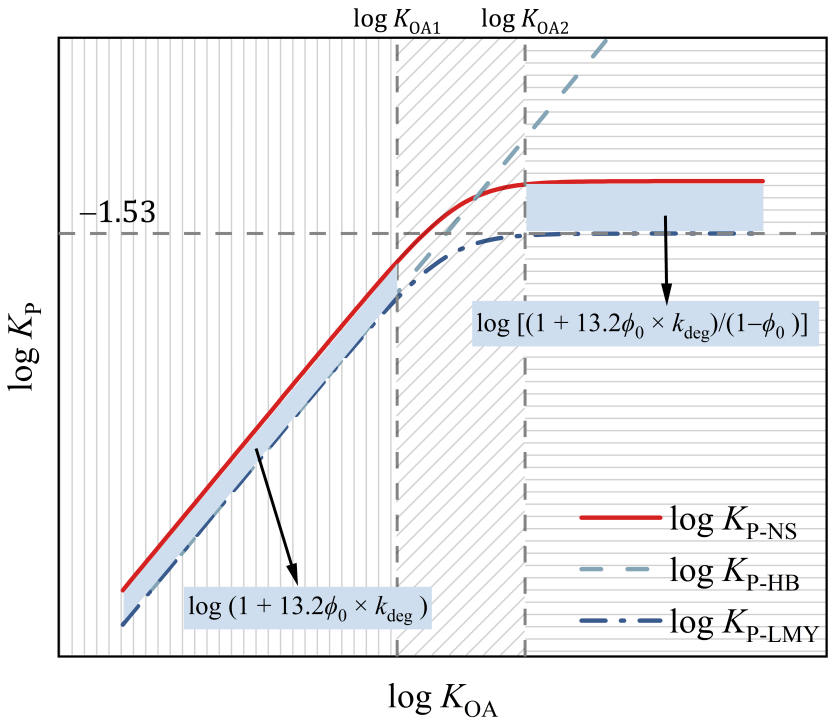


Fig. 2. The three domains of the new steady-state G/P partitioning model divided by the two threshold values of log $K_{OA}$

### 3. Influence of $\phi_0$ on $K_P$ of PAHs

In general, the different values of $\phi_0$ are corresponding to different forms of the new steady-state model (Eq. (3)). Three different forms can be obtained under different values of $\phi_0$ ($0 < \phi_0 < 1$, $\phi_0 = 0$, and $\phi_0 = 1$).

When $0 < \phi_0 < 1$, the particle phase and gas phase PAHs both exist in the emission, and the new steady-state model is expressed as Eq. (3). In this form, the gaseous interference and the particulate interference all need to be considered for the G/P partitioning of PAHs in atmosphere. The deviation of the new steady-state model from the H-B model, depends on the ratio of $\phi_0 D_{GR}$ to $(1 - \phi_0)(D_{PD} + D_{PW})$. When the ratio was higher than 1, the log $K_{P\text{-}NS}$ presented upwards from the prediction of the H-B model, while the log $K_{P\text{-}NS}$ presented downwards, when the ratio was lower than 1.

When $\phi_0 = 0$, the PAHs in the emission is totally gaseous PAHs, and the Eq. (3) is expressed as follows:

$$\log K_{P-NS} = \log K_{P-HB} + \log\left(\frac{D_{GP}}{D_{GP}+(D_{PD}+D_{PW})}\right) \quad (10)$$

In fact, this equation is identical to that of the L-M-Y model, where $\alpha = D_{GP} / (D_{GP} + D_{PD} + D_{PW})$ (Li et al., 2015).

When $\phi_0 = 1$, the PAHs in the emission is totally particulate PAHs, and the Eq. (3) is expressed as follows:

$$\log K_{P-NS} = \log K_{P-HB} + \log\left(\frac{D_{GP}+D_{GR}}{D_{GP}}\right) \quad (11)$$

The ~~derivation~~deviation of the new steady-state model from the H-B model was mainly caused by the degradation of PAHs in gas phase. When $k_{deg}$ is small enough to be ignored, the new steady-state model is equal to the H-B model.

The specific influence of $\phi_0$ on $K_{P\text{-}NS}$ of PAHs was studied with different values of $\phi_0$, and the results are showed in **Fig. 3**. As exhibited in **Fig. 3a**, the prediction line of the new steady-state model diverged from the L-M-Y model to the H-B model with the

increasing of $\phi_0$, which was consistent with the results reported in previous studies (Zhao et al., 2020; Qin et al., 2021). In addition, obvious differences were observed between the prediction lines for the three models. In particular, when $\phi_0 = 1$, the line of log $K_{P\text{-}NS}$ was parallel with the line of log $K_{P\text{-}HB}$. When $\phi_0 = 0$, the prediction line of log $K_{P\text{-}NS}$ was same with that of log $K_{P\text{-}LMY}$. When $0 < \phi_0 < 1$, the trends of the prediction lines of log $K_{P\text{-}NS}$ were similar to that of log $K_{P\text{-}LMY}$. The deviations between the prediction lines of log $K_{P\text{-}NS}$ and log $K_{P\text{-}LMY}$ are showed in **Fig. 3b**. In general, the deviations between the prediction lines varied with the values of $\phi_0$ and log $K_{OA}$. In addition, the deviation became larger along with the increase of $\phi_0$. And the deviation exhibited three different trends along with the increasing of log $K_{OA}$ separated by the two threshold values of log $K_{OA}$ (log $K_{OA1}$ and log $K_{OA2}$).

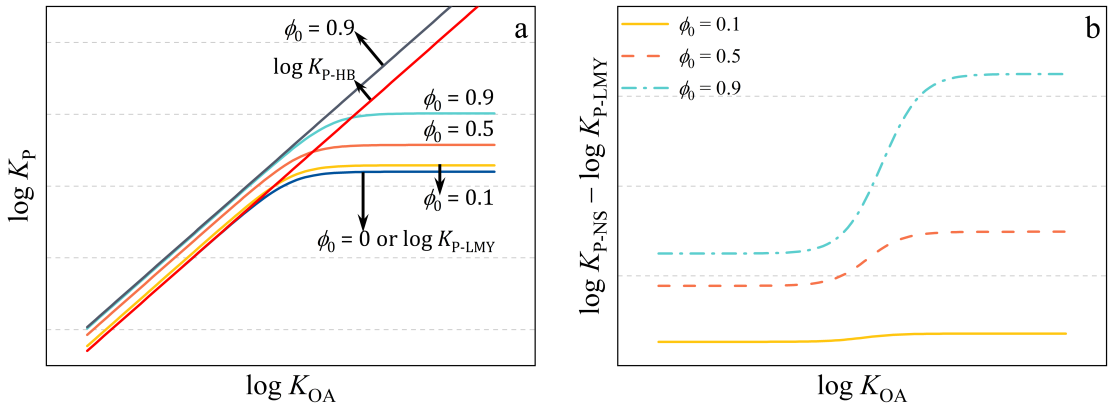


Fig. 3. The comparison between the new steady-state model and the H-B model and the L-M-Y model (Note: a, the prediction lines of the three models; b, the difference between the new steady-state model and the L-M-Y model with different values of $\phi_0$.)

## 4. Validation of the new steady-state G/P partitioning model

### 4.1. Validation

As we know, the emission sources of PAHs in atmosphere is complex, including stationary sources and mobile sources (Zhang et al., 2020). Furthermore, various proportions of particulate PAHs were also reported in different emission sources

(Zimmerman et al., 2019; Wang et al., 2018b; Shen et al., 2011; Cai et al., 2018b). Therefore, the precise values of $\phi_0$ cannot be easily confirmed. In this section, the different values of $\phi_0$ (0, 0.1, 0.5, 0.9, 0.99, and 1) were considered with the new steady-state model for the prediction of $K_{P\text{-}M}$ of PAHs in order to obtain representative results.

In order to evaluate the performance of the new steady-state model, the monitored values of the log $K_{P\text{-}M}$ of PAHs from 11 cities across China were applied (Ma et al., 2018; Ma et al., 2019; Ma et al., 2020). As showed in **Fig. 4**, the prediction line of the new steady-state model matched well with the monitoring data of log $K_{P\text{-}M}$. Especially for the monitoring data with high log $K_{OA}$, the data mainly distributed between the prediction lines of the steady-state model with the values of $\phi_0$ from 0 to 1. In addition, for different cities (**Fig. S3, SI**), the values of $\phi_0$ for the best matched prediction lines of the new steady-state model were different, which was expected since the sources of PAHs were also different among the 11 cities. The matching degree of the new steady-state model was also evaluated by the method of the root mean square error (*RMSE*, **Text S5, SI**). In general, for PAHs with high~~er~~ values of log $K_{OA}$ (such as the high molecular weight PAHs), when $\phi_0$ were 0.9 or 0.99, the value of *RMSE* for each city was the lowest (**Fig. S4, SI**), which indicated the best matching degree between the prediction results and the monitoring results. Actually, previous studies found that high molecular weight PAHs were dominant in particle phase in emissions with higher $\phi_0$ (Shen et al., 2011; Mastral et al., 1996; Lu et al., 2009), which indicated that our findings were reasonable.

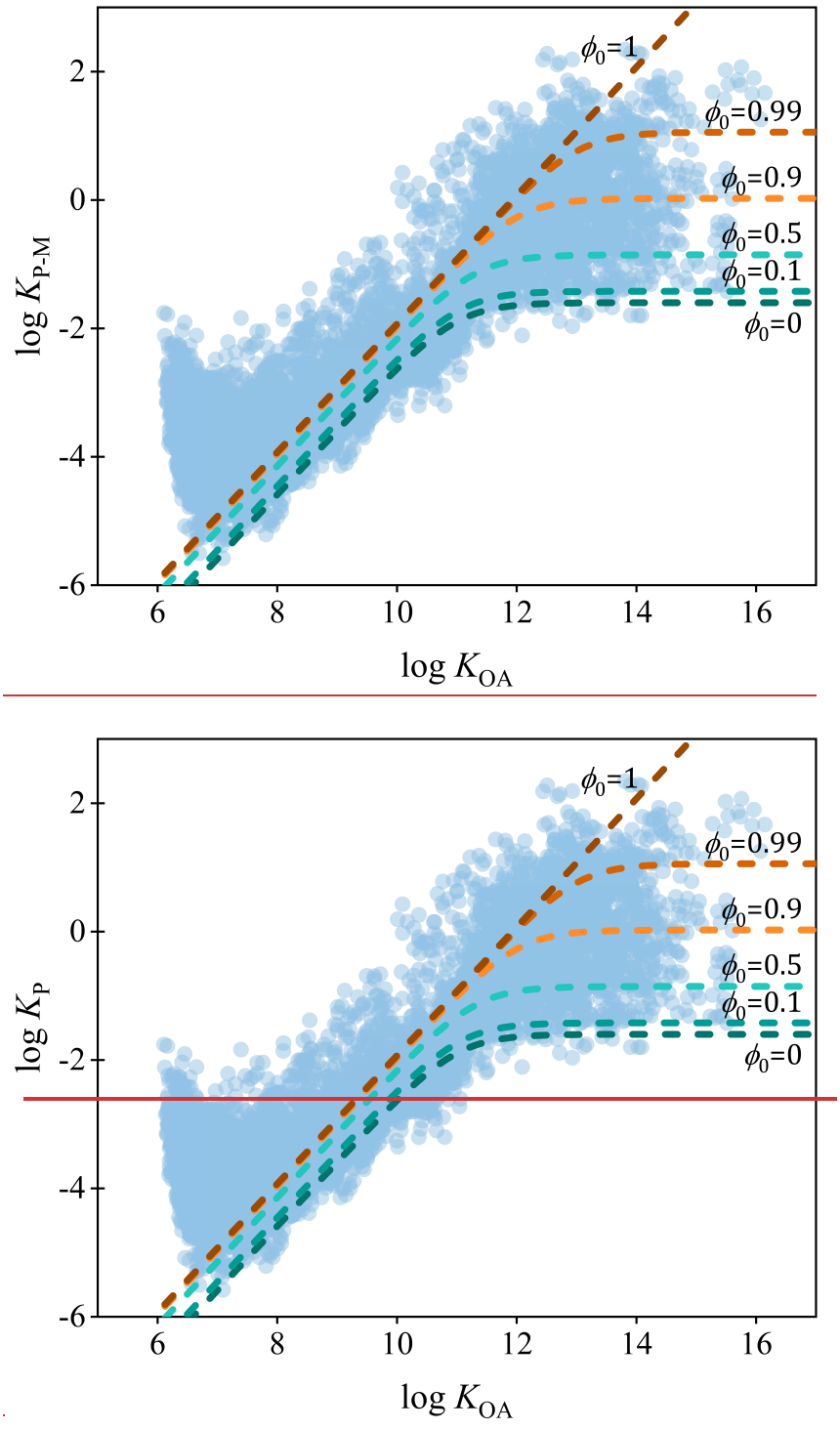


Fig. 4. The comparison between the monitored data of log $K_{P\text{-}M}$ of PAHs from 11 cities in China and the prediction lines of the new steady-state model with different values of $\phi_0$

Furthermore, the performance of the new steady-state model for the prediction of log $K_{P\text{-}M}$ of PAHs in special scenario was also discussed. It was found that in the prototype coking plant, the removal efficiency of dust was 96% (Liu et al., 2019). In

this scenario, the gaseous PAHs dominated in the emission, and the values of $\phi_0$ can be considered as ~0. As showed in **Fig. S5, SI**, the monitored data of log $K_{P\text{-}M}$ from the coking plant matched best with the prediction line of the new steady-state model with $\phi_0 = 0$, with the lowest *RMSE*. According to the comparison, the best matched $\phi_0$ in the steady-state model was consistent with that in the emission profile. The results indicated the good performance of the new steady-state model in this special scenario.

Furthermore, although the model was developed based on the parameters of PAHs, taking into account comparable partitioning characteristics of SVOCs, the steady-state model could be expanded to other SVOCs. A special scenario with the recycling of electrical and electronic waste site (E-waste site) was considered to validate the performance of the new steady-state model for other SVOCs. In this case, PBDEs were mainly in particle phase in the emissions, and the values of $\phi_0$ can be considered as ~1 (Cai et al., 2018a). **Fig. S6, SI** illustrates the comparison between the monitored data of log $K_{P\text{-}M}$ from several E-waste sites (Tian et al., 2011; Han et al., 2009; Chen et al., 2011) and the prediction lines of the new steady-state model with different values of $\phi_0$ (0, 0.1, 0.5, 0.9, 0.99, and 1). The related results for *RMSE* are showed in **Fig. S7, SI**. It is interesting to note that the monitored data of log $K_{P\text{-}M}$ matched best with the prediction line of the new steady-state model with $\phi_0 = 1$, which also had the lowest values of *RMSE*. Therefore, it can be concluded that the new steady-state model could be expanded to the prediction of $K_{P\text{-}M}$ of PBDEs in E-waste sites.

### 4.2. Implication

The present study has established a new steady-state G/P partitioning model, which takes into account the particulate proportion of SVOCs in emission. In summary, the study provided a new insight for the field of G/P partitioning and other related fields with SVOCs. Firstly, if the SVOCs in atmosphere are from diverse sources of emissions

with different $\phi_0$, the new steady-state model is much more suitable for the G/P partitioning study and related studies, such as health risk assessment. Secondly, when studying the pollution characteristic and regional transport of SVOCs from a single point source, such as the transport of PBDEs around an E-waste site or the transport of SVOCs around chemical factories, the G/P partitioning of SVOCs must take into account the particulate proportion of SVOCs in emissions. Thirdly, for long-range atmospheric transport studies, if there are various sources of SVOCs along the transport route, the continuous effect of the particulate proportion of SVOCs in emissions on the transport and fate of SVOCs requires careful consideration, such as the establishment of atmospheric transport model.

### 4.3. Limitation

Based on the above discussion, it can be concluded that the new steady-state model had good performance for the prediction of $K_{P\text{-}M}$ of PAHs in various real atmospheres, which provided a new method for the studying on the G/P partitioning of PAHs and other SVOCs. However, some limitations of the new steady-state model still existed in the present study. First, the values of $\phi_0$ were different between different compounds and different emission sources (Zimmerman et al., 2019; Wang et al., 2018b; Shen et al., 2011; Cai et al., 2018b). In ~~this~~ the present study, some constant values of $\phi_0$ were used for the new steady-state model, which was only ~~can~~ be considered as special examples. The exact values of $\phi_0$ should be used for the application of the new steady-state model in future. Second, for the gaseous degradation ($k_{deg}$) and the fraction of the organic matter in particle ($f_{OM}$), only one constant and common value was used for the new steady-state model. In general, these two parameters were also complicated in real atmosphere. For example, the $k_{deg}$ was not only related to the physicochemical properties of chemicals, but also related to the environmental parameters, such as

temperature and concentration (Wilson et al., 2020). In addition, even though the $f_{OM}$ can be directly measured, the actual values of $f_{OM}$ also changed along with many factors, such as emission sources (Gaga and Ari, 2019; Lohmann and Lammel, 2004) and particle sizes (Hu et al., 2020). In order to evaluate the influence of the three parameters on the $K_{P\text{-}NS}$ in the new steady-state model, the sensitivity analysis was conducted by the Monte Carlo analysis with 100,000 trials using the commercial software package Oracle Crystal Ball. In order to obtain comprehensive results, the sensitivity analysis was conducted for different values of log $K_{OA}$ from 6 to 16. As presented in **Fig. S8, SI**, it is interesting to note that three different ranges of log $K_{OA}$ were observed according to the different characteristics. For the range of log $K_{OA}$ from 6 to 10, the influence of $\phi_0$ was the dominant followed by $k_{deg}$ and $f_{OM}$. Furthermore, for each parameter, the influence was stable for different log $K_{OA}$ in range. For the range of log $K_{OA}$ from 10 to 12, the influence of $\phi_0$ was also the dominant followed by $k_{deg}$ and $f_{OM}$. In addition, the influence of $\phi_0$ increased, while for the other two parameters the influence decreased. In the third range of log $K_{OA}$ (12 to 16), the influences of the three parameters were also stable. In addition, the influence of $\phi_0$ was also the dominant, and the influence of $f_{OM}$ can be ignored. Actually, the three ranges of log $K_{OA}$ were consistent with the three domains. It can be concluded that the different influences of the three parameters on $K_{P\text{-}NS}$ for different log $K_{OA}$ should be considered for the new model. Therefore, the exact values of $\phi_0$, $k_{deg}$ and $f_{OM}$ for the real atmosphere should ~~also~~ be used for the application of the new steady-state model in future.

~~Third~~Furthermore, the new steady-state model was established based on a single multimedia environment, in which the advections of air and water were not considered. In addition, some fluxes were removed in order to simplify the parameters of the model. Therefore, the influence of all fluxes and parameters related to gas and particle

compartments should be evaluated comprehensively in future. Furthermore, the validation and implication of the new steady-state G/P partitioning model should also be conducted for other SVOCs in real multimedia environment.

## Author Contribution

**Fu-Jie Zhu**: Methodology, Investigation, Writing - original draft preparation. **Peng-Tuan Hu**: Writing - review & editing. **Wan-Li Ma**: Conceptualization, Methodology, Writing - review & editing.

## Competing interests

The authors declare that they have no conflict of interest.


## Acknowledgments

This study was supported by the National Natural Science Foundation of China (No. 41671470 and No. 42077341). This study was partially supported by the State Key Laboratory of Urban Water Resource and Environment, Harbin Institute of Technology (No. ~~2020TS03~~2023TS18) and the Heilongjiang Touyan Innovation Team Program, China.

## References


Bidleman, T. F.: Atmospheric processes wet and dry deposition of organic compounds are controlled by their vapor-particle partitioning, Environ. Sci. Technol., 22, 361-367, https://doi.org/10.1021/es00169a002, 1988.

Cai, C., Yu, S., Liu, Y., Tao, S., and Liu, W.: PBDE emission from E-wastes during the pyrolytic process: Emission factor, compositional profile, size distribution, and gas-particle partitioning, Environ. Pollut., 235, 419-428, http://doi.org/10.1016/j.envpol.2017.12.068, 2018a.

Cai, C., Yu, S., Li, X., Liu, Y., Tao, S., and Liu, W.: Emission characteristics of polycyclic aromatic hydrocarbons from pyrolytic processing during dismantling of electronic wastes, J. Hazard. Mater., 351, 270-276, http://doi.org/10.1016/j.jhazmat.2018.03.012, 2018b.

Chen, D., Bi, X., Liu, M., Huang, B., Sheng, G., and Fu, J.: Phase partitioning, concentration variation and risk assessment of polybrominated diphenyl ethers (PBDEs) in the atmosphere of an e-waste recycling site, Chemosphere, 82, 1246-1252, https://doi.org/10.1016/j.chemosphere.2010.12.035, 2011.

Dachs, J. and Eisenreich, S. J.: Adsorption onto aerosol soot carbon dominates gas-particle partitioning of polycyclic aromatic hydrocarbons, Environ. Sci. Technol., 34, 3690-3697, https://doi.org/10.1021/es991201+, 2000.

Gaga, E. O. and Ari, A.: Gas-particle partitioning and health risk estimation of polycyclic aromatic hydrocarbons (PAHs) at urban, suburban and tunnel atmospheres: Use of measured EC and OC in model calculations, Atmospheric Pollution Research, 10, 1-11, http://doi.org/10.1016/j.apr.2018.05.004, 2019.

Goss, K.-U.: Predicting the equilibrium partitioning of organic compounds using just one linear solvation energy relationship (LSER), Fluid Phase Equilib., 233, 19-22, https://doi.org/10.1016/j.fluid.2005.04.006, 2005.

Han, W., Feng, J., Gu, Z., Chen, D., Wu, M., and Fu, J.: Polybrominated Diphenyl Ethers in the Atmosphere of Taizhou, a Major E-Waste Dismantling Area in China, Bul. Environ. Contam. Toxicol., 83, 783-788, https://doi.org/10.1007/s00128-009-9855-9, 2009.

Harner, T. and Bidleman, T. F.: Octanol-air partition coefficient for describing particle/gas partitioning of aromatic compounds in urban air, Environ. Sci. Technol., 32, 1494-1502, https://doi.org/10.1021/es970890r, 1998.

Hu, P.-T., Ma, W.-L., Zhang, Z.-F., Liu, L.-Y., Song, W.-W., Cao, Z.-G., Macdonald, R. W., Nikolaev, A., Li, L., and Li, Y.-F.: Approach to Predicting the Size-Dependent Inhalation Intake of Particulate Novel Brominated Flame Retardants, Environ. Sci. Technol., 55, 15236-15245, https://doi.org/10.1021/acs.est.1c03749, 2021.

Hu, P.-T., Su, P.-H., Ma, W.-L., Zhang, Z.-F., Liu, L.-Y., Song, W.-W., Qiao, L.-N., Tian, C.-G., Macdonald, R. W., Nikolaev, A., Cao, Z.-G., and Li, Y.-F.: New equation to predict size-resolved gas-particle partitioning quotients for polybrominated diphenyl ethers, J. Hazard. Mater., 400, 123245, https://doi.org/10.1016/j.jhazmat.2020.123245, 2020.

Hung, H., Blanchard, P., Halsall, C. J., Bidleman, T. F., Stern, G. A., Fellin, P., Muir, D. C. G., Barrie, L. A., Jantunen, L. M., Helm, P. A., Ma, J., and Konoplev, A.: Temporal and spatial variabilities of atmospheric polychlorinated biphenyls (PCBs), organochlorine (OC) pesticides and polycyclic aromatic hydrocarbons (PAHs) in the Canadian Arctic: Results from a decade of monitoring, Science of the Total Environment, 342, 119-144, https://doi.org/10.1016/j.scitotenv.2004.12.058, 2005.

Hung, H., Kallenborn, R., Breivik, K., Su, Y., Brorström-Lundén, E., Olafsdottir, K., Thorlacius, J. M., Leppänen, S., Bossi, R., Skov, H., Manø, S., Patton, G. W., Stern, G., Sverko, E., and Fellin, P.: Atmospheric monitoring of organic pollutants in the Arctic under the Arctic Monitoring and Assessment Programme (AMAP): 1993–2006, Science of the Total Environment, 408, 2854-2873, https://doi.org/10.1016/j.scitotenv.2009.10.044, 2010.

Li, Y., Ma, W., and Yang, M.: Prediction of gas/particle partitioning of polybrominated diphenyl ethers (PBDEs) in global air: A theoretical study, Atmospheric Chemistry and Physics, 15, 1669-1681, https://doi.org/10.5194/acp-15-1669-2015, 2015.

Li, Y. F. and Jia, H. L.: Prediction of gas/particle partition quotients of Polybrominated Diphenyl Ethers (PBDEs) in north temperate zone air: An empirical approach, Ecotoxicology & Environmental Safety, 108, 65-71, https://doi.org/10.1016/j.ecoenv.2014.05.028, 2014.

Liu, X., Zhao, D., Peng, L., Bai, H., Zhang, D., and Mu, L.: Gas–particle partition and spatial characteristics of polycyclic aromatic hydrocarbons in ambient air of a prototype coking plant, Atmos. Environ., 204, 32-42, https://doi.org/10.1016/j.atmosenv.2019.02.012, 2019.

Lohmann, R. and Lammel, G.: Adsorptive and Absorptive Contributions to the Gas-Particle Partitioning of Polycyclic Aromatic Hydrocarbons: State of Knowledge and Recommended Parametrization for Modeling, Environ. Sci. Technol., 38, 3793-3803, https://doi.org/10.1021/es035337q, 2004.

Lu, H., Zhu, L., and Zhu, N.: Polycyclic aromatic hydrocarbon emission from straw burning and the influence of combustion parameters, Atmos. Environ., 43, 978-983, https://doi.org/10.1016/j.atmosenv.2008.10.022, 2009.

Ma, W., Zhu, F., Hu, P., Qiao, L., and Li, Y.: Gas/particle partitioning of PAHs based on equilibrium-state model and steady-state model, Sci. Total Environ., 706, 136029, https://doi.org/10.1016/j.scitotenv.2019.136029, 2020.

Ma, W.-L., Zhu, F.-J., Liu, L.-Y., Jia, H.-L., Yang, M., and Li, Y.-F.: PAHs in Chinese atmosphere: Gas/particle partitioning, Sci. Total Environ., 693, 133623, https://doi.org/10.1016/j.scitotenv.2019.133623, 2019.

Ma, W. L., Liu, L. Y., Jia, H. L., Yang, M., and Li, Y. F.: PAHs in Chinese atmosphere Part I: Concentration, source and temperature dependence, Atmos. Environ., 173, 330-337, https://doi.org/10.1016/j.atmosenv.2017.11.029, 2018.

Mastral, A. M., Callén, M., and Murillo, R.: Assessment of PAH emissions as a function of coal combustion variables, Fuel, 75, 1533-1536, https://doi.org/10.1016/0016-2361(96)00120-2, 1996.

Pankow, J. F.: Review and comparative analysis of the theories on partitioning between the gas and aerosol particulate phases in the atmosphere, Atmos. Environ., 21, 2275-2283, https://doi.org/10.1016/0004-6981(87)90363-5, 1987.

Qiao, L., Hu, P., Macdonald, R., Kannan, K., Nikolaev, A., and Li, Y.-f.: Modeling gas/particle partitioning of polybrominated diphenyl ethers (PBDEs) in the atmosphere: A review, Sci. Total Environ., 729, 138962, https://doi.org/10.1016/j.scitotenv.2020.138962, 2020.

Qiao, L., Zhang, Z., Liu, L., Song, W., Ma, W., Zhu, N., and Li, Y.: Measurement and modeling the gas/particle partitioning of organochlorine pesticides (OCPs) in atmosphere at low temperatures, Sci. Total Environ., 667, 318-324, http://doi.org/10.1016/j.scitotenv.2019.02.347, 2019.

Qin, M., Yang, P., Hu, P., Hao, S., Macdonald, R. W., and Li, Y.: Particle/gas partitioning for semi-volatile organic compounds (SVOCs) in level III multimedia fugacity models: Both gaseous and particulate emissions, Sci. Total Environ., 790, 148012, https://doi.org/10.1016/j.scitotenv.2021.148012, 2021.

Shahpoury, P., Lammel, G., Albinet, A., Sofuoglu, A., Dumanoglu, Y., Sofuoglu, S. C., Wagner, Z., and Zdimal, V.: Evaluation of a conceptual model for gas-particle partitioning of polycyclic aromatic hydrocarbons using polyparameter linear free energy relationships, Environ. Sci. Technol., 50, 12312-12319, https://doi.org/10.1021/acs.est.6b02158, 2016.

Shen, G., Wang, W., Yang, Y., Ding, J., Xue, M., Min, Y., Zhu, C., Shen, H., Li, W., Wang, B., Wang, R., Wang, X., Tao, S., and Russell, A. G.: Emissions of PAHs from indoor crop residue burning in a typical rural stove: Emission factors, size distributions, and

gas−particle partitioning, Environ. Sci. Technol., 45, 1206-1212, https://doi.org/10.1021/es102151w, 2011.
Tang, T., Cheng, Z., Xu, B., Zhang, B., Zhu, S., Cheng, H., Li, J., Chen, Y., and Zhang, G.: Triple Isotopes (delta C-13, delta H-2, and Delta C-4) Compositions and Source Apportionment of Atmospheric Naphthalene: A Key Surrogate of Intermediate-Volatility Organic Compounds (IVOCs), Environ. Sci. Technol., 54, 5409-5418, https://doi.org/10.1021/acs.est.0c00075, 2020.
Tian, M., Chen, S.-J., Wang, J., Zheng, X.-B., Luo, X.-J., and Mai, B.-X.: Brominated Flame Retardants in the Atmosphere of E-Waste and Rural Sites in Southern China: Seasonal Variation, Temperature Dependence, and Gas-Particle Partitioning, Environ. Sci. Technol., 45, 8819-8825, https://doi.org/10.1021/es202284p, 2011.
Vuong, Q. T., Thang, P. Q., Nguyen, T. N. T., Ohura, T., and Choi, S. D.: Seasonal variation and gas/particle partitioning of atmospheric halogenated polycyclic aromatic hydrocarbons and the effects of meteorological conditions in Ulsan, South Korea, Environ. Pollut., 263, https://doi.org/10.1016/j.envpol.2020.114592, 2020.
Wang, C., Wang, X., Gong, P., and Yao, T.: Long-term trends of atmospheric organochlorine pollutants and polycyclic aromatic hydrocarbons over the southeastern Tibetan Plateau, Science of the Total Environment, 624, 241-249, https://doi.org/10.1016/j.scitotenv.2017.12.140, 2018a.
Wang, R., Liu, G., Sun, R., Yousaf, B., Wang, J., Liu, R., and Zhang, H.: Emission characteristics for gaseous- and size-segregated particulate PAHs in coal combustion flue gas from circulating fluidized bed (CFB) boiler, Environ. Pollut., 238, 581-589, https://doi.org/10.1016/j.envpol.2018.03.051, 2018b.
Wei, X., Yuan, Q., Serge, B., Xu, T., Ma, G., and Yu, H.: In silico investigation of gas/particle partitioning equilibrium of polybrominated diphenyl ethers (PBDEs), Chemosphere, 188, 110-118, http://doi.org/10.1016/j.chemosphere.2017.08.146, 2017.
Weschler, C. J., Beko, G., Koch, H. M., Salthammer, T., Schripp, T., Toftum, J., and Clausen, G.: Transdermal Uptake of Diethyl Phthalate and Di(n-butyl) Phthalate Directly from Air: Experimental Verification, Environ. Health Perspect., 123, 928-934, https://doi.org/10.1289/ehp.1409151, 2015.
Wilson, J., Pöschl, U., Shiraiwa, M., and Berkemeier, T.: Non-equilibrium interplay between gas-particle partitioning and multiphase chemical reactions of semi-volatile compounds: mechanistic insights and practical implications for atmospheric modeling of PAHs, Atmospheric Chemistry and Physics, 2020, 1-39, https://doi.org/10.5194/acp-21-6175-2021, 2020.
Zhang, L., Yang, L., Zhou, Q., Zhang, X., Xing, W., Wei, Y., Hu, M., Zhao, L., Toriba, A., Hayakawa, K., and Tang, N.: Size distribution of particulate polycyclic aromatic hydrocarbons in fresh combustion smoke and ambient air: A review, Journal of Environmental Sciences, 88, 370-384, https://doi.org/10.1016/j.jes.2019.09.007, 2020.
Zhao, F., Riipinen, I., and MacLeod, M.: Steady-state mass balance model for predicting particle–gas concentration ratios of PBDEs, Environ. Sci. Technol., 55, 9425-9433, https://doi.org/10.1021/acs.est.0c04368, 2020.
Zhu, F.-J., Ma, W.-L., Zhang, Z.-F., Yang, P.-F., Hu, P.-T., Liu, L.-Y., and Song, W.-W.: Prediction of the gas/particle partitioning quotient of PAHs based on ambient temperature, Sci. Total Environ., 811, 151411, https://doi.org/10.1016/j.scitotenv.2021.151411, 2021.
Zhu, F.-J., Ma, W.-L., Zhang, Z.-F., Yang, P.-F., Hu, P.-T., Liu, L.-Y., and Song, W.-W.: Prediction of the gas/particle partitioning quotient of PAHs based on ambient temperature, Sci. Total Environ., 811, 151411, https://doi.org/10.1016/j.scitotenv.2021.151411, 2022.
Zimmerman, N., Rais, K., Jeong, C.-H., Pant, P., Mari Delgado-Saborit, J., Wallace, J. S., Evans, G. J., Brook, J. R., and Pollitt, K. J. G.: Carbonaceous aerosol sampling of gasoline direct

injection engine exhaust with an integrated organic gas and particle sampler, Sci. Total Environ., 652, 1261-1269, https://doi.org/10.1016/j.scitotenv.2018.10.332, 2019.